

Implementation Issues of A Wideband Multi-Resolution Spectrum Sensing (MRSS) Technique for Cognitive Radio (CR) Systems

J. Park¹, Y. Hur², T. J. Song¹, K. Kim¹, J. Lee³, K. Lim¹, C.-H. Lee², H. S. Kim⁴, and J. Laskar¹

¹ Georgia Electronic Design Center (GEDC), Georgia Institute of Technology, Atlanta, GA, USA

² Samsung RFIC Design Center at Georgia Tech., Atlanta, GA, USA

³ Samsung Electro-Mechanics Inc., Suwon, Korea

⁴ Hanbat National University, Daejeon, Korea

park@gatech.edu

Abstract

Spectrum sensing is a key function for a Cognitive Radio (CR) system. An analog-based Multi-Resolution Spectrum Sensing (MRSS) technique was proposed as a flexible, low-power, high-speed spectrum-sensing solution. In this paper, implementation issues of the MRSS technique are investigated, and the corresponding practical specifications are suggested. First, nonlinear effects from a Voltage-Controlled Oscillator (VCO) and multipliers are explored. System simulation results show that harmonic distortion components of VCO and wavelet-pulse power levels should be controlled to alleviate these nonlinear effects. Afterward, I/Q phase- and gain-mismatch effects are addressed. Specifically, narrow-band signals are more sensitive to these gain and phase mismatches compared to broadband digital modulated signals. Overall, phase mismatch is more sensitive than gain mismatch on MRSS performance, showing a linear degradation of a detected power-level up to a 60-degree phase-mismatch.

1. Introduction

With the ever-growing need for wireless communications, wireless spectrum resources have been exhausted. Recently, Cognitive Radio (CR) technology has been proposed to increase the efficiency of spectrum utilization [1, 2]. Depending on time and location, some of the licensed spectrum resources are not fully exploited by primary users [3, 4]. By adopting the dynamic spectrum resource management concept, the CR system aims to use unoccupied spectrum segments, while guaranteeing the right of privileged primary users [3, 5].

The spectrum sensing technique is key functionality for identifying the spectrum usage status over a wide frequency range covering various communication standards. Its most critical performance requirements are accuracy and time of spectrum sensing. Moreover, low power consumption and simple implementation are desired from the commercialization viewpoint of CR systems.

Various spectrum-sensing methods have been proposed so far [6-9]. They can be categorized into two groups, i.e. energy

detection [6, 7] and feature detection [8, 9]. The energy detection method enables fast sensing-speed and simple implementation. However, as its sensing accuracy depends on selection of the threshold level, its performance is vulnerable to noise and noise-like broadband digital modulated signals. Meanwhile, the feature detection method [8, 9] is designed to identify the corresponding signature feature of each signal modulation type. However, this method requires longer processing time and excessive digital hardware resources accompanying large power consumption.

The IEEE 802.22 working group is developing a Wireless Regional Area Network (WRAN) standard based on CR technology utilizing TV broadcasting spectrum resources (i.e. VHF and UHF band). A dual-stage spectrum sensing scheme [10] was suggested to meet these requirements mentioned above. First of all, an energy detection method, the Multi-Resolution Spectrum Sensing (MRSS) technique [11], takes a snapshot of the current spectrum usage pattern. Specifically, this MRSS technique identifies the occupancy of each spectrum segment in a fast but sparse manner. Subsequently, a time-domain feature detection method scrutinizes the candidate spectrum segments determined safe from the MRSS stage. This sensing stage ensures that no primary users are interfered by detecting even noise-level signal features that are unique for each modulation type.

In this paper, analog low-power implementation issues of the MRSS technique are investigated. In Section 2, theoretical backgrounds of the MRSS technique are briefly introduced. Sections 3 and 4 address its implementation issues such as nonlinear effects and I/Q mismatches, respectively. From thorough system simulations, the corresponding practical specifications of each building block are investigated and suggested.

2. A wideband MRSS technique

Wavelet transforms have various choices of basis functions, some of which have a resolution bandwidth as an additional freedom-of-design [12]. A wavelet transform coefficient is obtained from the correlation between a given signal and a specific wavelet-basis waveform. Therefore, by adjusting this wavelet's pulse width and its carrier frequency, spectral

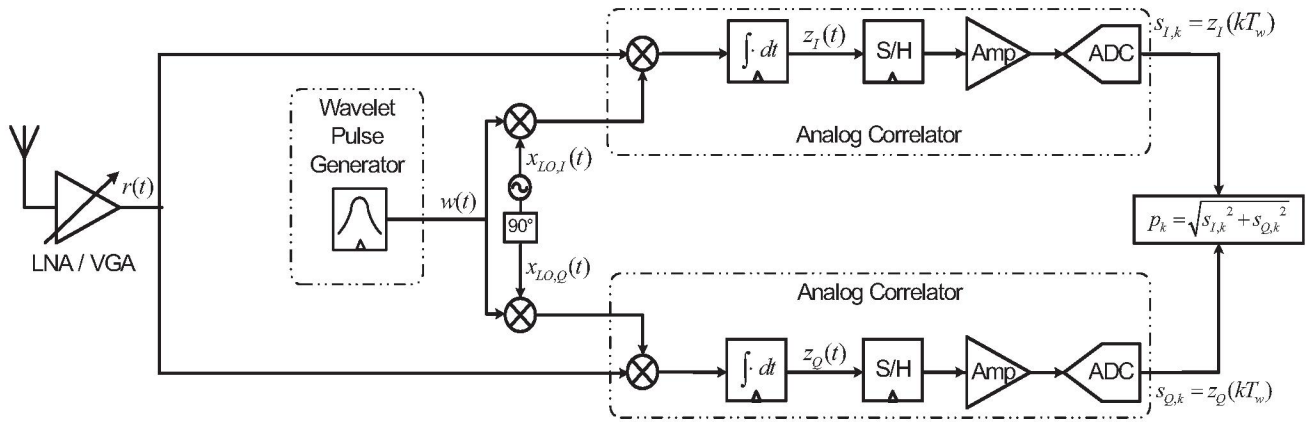


Figure 1. Functional block diagram of the suggested MRSS technique

contents can be represented with a scalable resolution or multi-resolution.

Fig. 1 shows the functional block diagram of the suggested MRSS technique. Building blocks consist of a wavelet pulse generator and analog correlators. Specifically, this analog correlator is composed of a multiplier, an integrator circuit, a Sample-and-Hold (S/H) circuit, an amplifier and ADC. Since the MRSS processing is performed in the analog domain, low-power and real-time operations are realizable. Moreover, a wavelet pulse provides a band-pass filtering effect for noisy RF input signals. Thus, image- and noise-rejection filters are not required.

A wavelet pulse generator generates the wavelet basis $w(t)$ of the predetermined shape with the pulse width of T_w . By changing this T_w , spectrum-sensing resolution-bandwidth, B_w , is adjusted. The frequency span ($f_{stop} - f_{start}$) is investigated by sweeping f_k with the increment of f_{sweep} . For each frequency f_k , analog correlators calculate the spectral contents $z_I(t)$ and $z_Q(t)$ of $r(t)$, as shown in (1-1) and (1-2), respectively.

$$z_I(t) = \frac{1}{2 \cdot T_w} \cdot \int_{k \cdot T_w}^{(k+1) \cdot T_w} [r(t) \cdot \{w(t) \cdot \cos(2\pi f_k t)\}] \cdot dt \quad (1-1)$$

$$z_Q(t) = \frac{1}{2 \cdot T_w} \cdot \int_{k \cdot T_w}^{(k+1) \cdot T_w} [r(t) \cdot \{w(t) \cdot \sin(2\pi f_k t)\}] \cdot dt \quad (1-2)$$

In the mean time, sinusoid signals or nonlinear multiplication may induce harmonic components in the process of correlation. These undesired terms from the nonlinear characteristics of a Voltage-Controlled Oscillator (VCO) and multipliers lead to the distorted correlation results. Furthermore, phase- and gain-mismatch of $z_I(t)$ and $z_Q(t)$ may cause unwanted terms of spectrum-sensing result.

Finally, the spectral magnitude p_k , represented with the given resolution-bandwidth B_w , is obtained at each frequency f_k as shown in (2).

$$p_k = \sqrt{z_I^2(kT_w) + z_Q^2(kT_w)} \quad (2)$$

This p_k is calculated with the discrete values sampled by ADCs with finite vertical resolution. Thus, the precision of the final spectrum sensing result depends on the vertical resolution of the ADCs.

For the verification of the MRSS spectrum sensing concept, a system simulation was performed for Frequency Modulation (FM), Orthogonal Frequency Division Multiplexing (OFDM) and 8-level Vestigial-Side Band (8-VSB) signals. The simulation conditions for each signal are summarized in Table I.

Fig. 2 shows the power spectrum of the input RF signal $r(t)$. Fig. 3(a) and 3(b) show the MRSS spectra detected in sparse (i.e. 20-MHz B_w , 20-MHz f_{sweep}) and precise (i.e. 2-MHz B_w , 2-MHz f_{sweep}) manner, respectively. In Fig. 3(a), the MRSS simulation result shows a wideband spectrum shape with blunt peaks for three input signals. Meanwhile, Fig. 3(b) shows three sharp peaks for each signal, indicating a better detection performance in terms of sensing resolution. Therefore, the suggested MRSS technique is able to examine a wideband spectrum in a fast sparse manner or, if needed, in a precise manner without any increase of hardware burden.

TABLE I
SIMULATION PARAMETERS FOR THE MRSS SIMULATION

Input Signals				
Modulation	Bandwidth	Carrier Freq.	Power	Remark
FM	200 KHz	170 MHz	- 65 dBm	Wireless Mic.
OFDM	7 MHz	333 MHz	- 37 dBm	DVB-T
8-VSB	6 MHz	600 MHz	- 58 dBm	ATSC

Simulation Parameters		
	Sparse MRSS	Precise MRSS
VCO Span	50 ~ 850 MHz	50 ~ 850 MHz
f_{sweep}	20 MHz	2 MHz
B_w	20 MHz	2 MHz
T_{total}	2.05 μ sec	200.5 μ sec

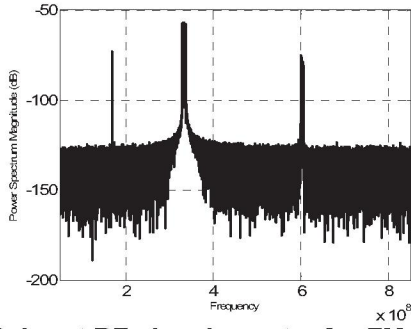


Figure 2. Input RF signal spectra for FM, OFDM and 8-VSB signals

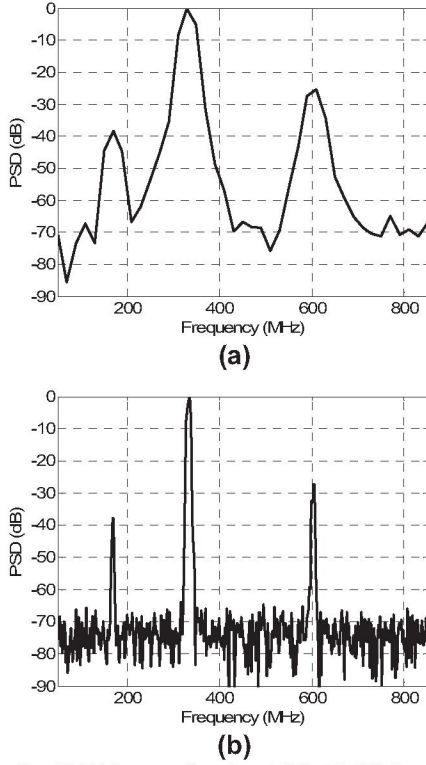


Figure 3. MRSS results for FM, OFDM and 8-VSB signals. (a) spectrum detected in a sparse manner (20-MHz B_w , 20-MHz f_{sweep}), (b) spectrum detected in a precise manner (2-MHz B_w , 2-MHz f_{sweep})

3. Nonlinear effects

In this chapter, nonlinear phenomena in a VCO and multipliers are investigated. Furthermore, their effects on MRSS performance are simulated for the conditions listed in the Table I.

3.1. VCO nonlinear effect

A VCO is employed to sweep the carrier frequency of the wavelet pulse in Fig. 1. Typically, this VCO generates multiple harmonics of the fundamental frequency f_k in (1). Specifically, the third-order harmonic component has the largest power level among all the harmonic components.

These spurious components of the VCO output signal may cause the undesired terms in the correlation results, as shown in (3).

$$z_I(t) + j \cdot z_Q(t) \approx \left(\frac{1}{2T_W} \right) \int_{kT_W}^{(k+1)T_W} [r(t) \{ w(t) \cdot VCO(t) \}] dt \quad (3)$$

, where $VCO(t) = e^{j2\pi f_k t} + \alpha_3 \cdot e^{j2\pi(3f_k)t}$, and α_3 is the magnitude of the third-order harmonic component of VCO output signal. These distortion terms from the third-order harmonic component may be larger than the threshold level regarded as the meaningful signal reception. Thus, the reliability of the MRSS technique may be affected and degraded by the nonlinear effect from the VCO harmonic responses.

Fig. 4 shows the simulation results of the VCO nonlinear effect on the MRSS result. With $\alpha_3 = 0.1$, the MRSS is performed for the input signal spectra in Fig. 2 with the precise sensing mode as in Fig. 3(b). Fig. 4 shows the corresponding MRSS result with the nonlinear effects of the VCO's third harmonic components. Additional peaks at 57, 112 and 200 MHz may be determined as the signal reception, depending on the threshold level. These erroneous sensing results may degrade the reliability of the MRSS technique. Therefore, the harmonic characteristics are critical specification of a VCO design for the MRSS implementation.

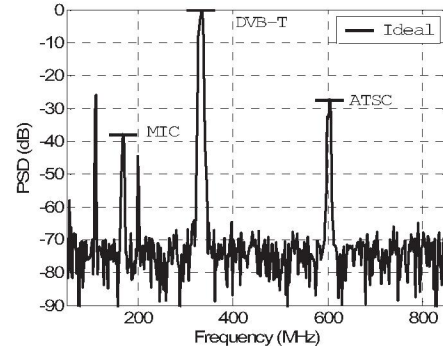


Figure 4. MRSS with the nonlinear effects of the third-order harmonic components of a VCO output

3.2. Multiplier nonlinear effect

Multipliers perform the mixing process of the signal with the wavelet-pulse signal. This mixing procedure generates the desired product term as well as the intermodulated terms. These intermodulation terms have wide range of frequency values. Some of these spurious terms fall in the high frequency range compared to the desired product term. These high-frequency spurs are filtered out with an integrator followed by the multiplier. Meanwhile, the intermodulation terms falling around DC can not be easily filtered out by the integrator. These low-frequency spurs may induce a DC-offset perturbation to the output of the integrator. As a result,

this DC-offset noise term affect the accuracy of the spectral magnitude, p_k .

A Gilbert-cell type multiplier is one of the commonly used topologies [13]. By adjusting the power of the wavelet pulse, spurious components of a multiplier output may be controlled. Fig. 5(a) and (b) show the spurious responses for different wavelet pulse power level, i.e. 0 dBm and -30 dBm, respectively. Fig. 5(b) shows smaller power levels of spurs than those in Fig. 5(a). These spur terms may affect the reliability of the MRSS technique. Thus, link budget of analog front-end implementation should consider this nonlinear effect of multipliers for MRSS performance.

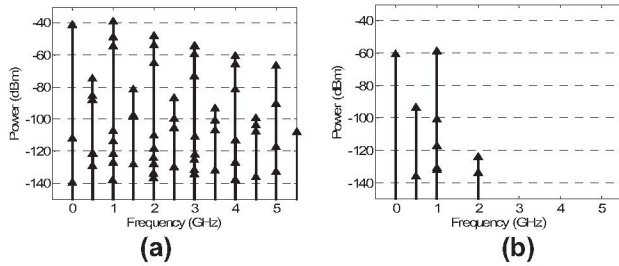


Figure 5. Simulated harmonic response of a Gilbert-cell type multiplier. RF signal is set to 501 MHz with the power of -30 dBm. LO signal is at 500 MHz with the power of (a) 0 dBm and (b) -30 dBm.

4. I/Q mismatch effect

In the MRSS technique, the spectral content of $r(t)$ is represented with the magnitude of two orthogonal components of the correlation, $z_I(t)$ and $z_Q(t)$. These two terms came from the wavelet pulses modulated with two orthogonal sinusoid carriers. Thus, I/Q-gain mismatch and phase-orthogonality error (i.e. phase mismatch), shown in (4), may affect the correlation values in (1).

$$x_{LO,I}(t) = \left(1 + \frac{\varepsilon}{2}\right) \cdot \cos\left(2\pi f_w t - \frac{\theta}{2}\right) \quad (4-1)$$

$$x_{LO,Q}(t) = \left(1 - \frac{\varepsilon}{2}\right) \cdot \sin\left(2\pi f_w t + \frac{\theta}{2}\right) \quad (4-2)$$

, where ε is a gain mismatch, and θ is a phase mismatch of the quadrature output of a VCO [13].

These I/Q gain- and phase-mismatch effects are investigated in this chapter. Furthermore, the corresponding performances are presented for each mismatch effect.

4.1. I/Q phase mismatch

The phase variation is large and fast for broadband modulated signals. Meanwhile, narrowband signal relatively experiences small phase variation within given time duration. Thus, phase orthogonality error pertains longer duration for

narrow band signal. In other words, narrow band signal such as FM signal is more vulnerable to this I/Q phase mismatch.

Fig. 6 shows the MRSS simulation result with 90-degree I/Q phase mismatch. In this simulation, input signal spectra in Fig. 2 were investigated with the precise sensing mode as in Fig. 3(b). Broadband modulated signals such as OFDM and 8-VSB are not sensitive to this extreme phase mismatch. Thus, those signals' spectra keep their original shape and values of the ideal I/Q phase case, as shown in Fig. 6. Meanwhile, with the increasing amount of phase mismatch, just FM signal's detected spectrum magnitude is decreasing, as shown in Fig. 6. Fig. 7 shows the degradation of a detected power of FM signals for the amount of I/Q phase mismatch. Up to 60-degree phase mismatch, the detected power level in dB-scale is decreasing linearly proportional to the phase mismatch.

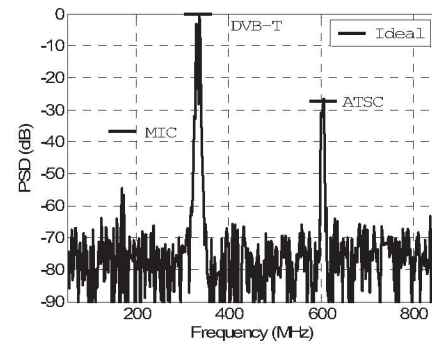


Figure 6. MRSS with 90-degree I/Q phase mismatch

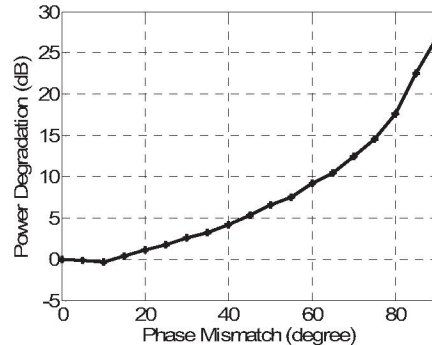


Figure 7. The degradation of a detected power of FM signals for the amount of I/Q phase mismatch

4.2. I/Q gain mismatch

I/Q gain-mismatch is the amount of gain- or loss-difference between I- and Q-channel signal paths. In the MRSS technique, the spectral content p_k is the magnitude of two orthogonal components of $z_I(kT_w)$ and $z_Q(kT_w)$, as shown in (2). The I/Q gain-mismatch ε emphasizes one of the contributions from $z_I(kT_w)$ and $z_Q(kT_w)$ to p_k . Thus, if the contribution to p_k is biased to one of I- and Q-component, this gain mismatch may distort the actual spectral value p_k , severely.

Narrow band signals such as FM signals have a tendency of biased contribution of I- or Q-component to p_k . Meanwhile, broadband digital modulation signals (i.e. OFDM, 8-VSB, WCDMA, etc.) have relatively complicated or, even, noise-like waveform shapes. Thus, there is little chance of having the biased correlation to one of I- or Q-component. In other words, the correlation contributions are almost evenly distributed to I- and Q-component. As a result, this I/Q gain-mismatch may affect narrowband signals more severely than broadband digital modulation signals.

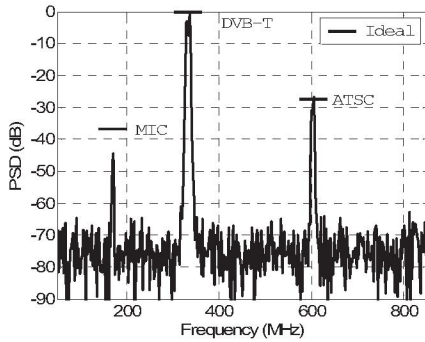


Figure 8. MRSS with 10-dB I/Q gain mismatch

Fig. 8 shows the result of MRSS with 10-dB I/Q-gain mismatch for the signal spectra shown in Fig. 2. The DVB-T (i.e. OFDM) and the ATSC (i.e. 8-VSB) signals, broadband digital modulated signals, are not affected by 10-dB I/Q-gain mismatch. Meanwhile, the detected spectrum power of FM signal is reduced by 7 dB.

Compared to the phase-mismatch, MRSS performance is immune to this gain-mismatch. Thus, phase orthogonality should be critical design specification in implementing quadrature-phase VCO for the MRSS technique.

5. Conclusion

The analog implementation of the suggested MRSS technique provides flexible spectrum-sensing resolution in a real-time, low-power operation. Theoretical backgrounds of the MRSS technique were introduced. Then, thorough system simulations were performed to investigate the non-ideal effects of analog building blocks on MRSS performance. Moreover, the corresponding specifications were suggested for the practical implementation of the MRSS technique.

The nonlinear responses of a VCO and multipliers were shown to produce undesired spurious responses. Thus, the third-order harmonics and wavelet-pulse power level should be controlled to alleviate these nonlinear effects.

Furthermore, the effect of I/Q gain- and phase-mismatch were examined on various modulation types of input signal. Narrowband signals were more sensitive to gain and phase mismatch compared to broadband signals. The MRSS technique was relatively immune to I/Q gain-mismatch compared to I/Q phase-mismatch. Thus, quadrature-phase

VCO should be optimized to keep I/Q phase orthogonal each other.

6. Acknowledgement

The authors wish to acknowledge Dr. W. Woo, Samsung RFIC Design Center at Georgia Tech., Atlanta, GA for his technical discussions.

7. References

- [1] Mitola, J., III, "Cognitive radio for flexible mobile multimedia communications," in Proc. IEEE Int. Workshop on Mobile Multimedia Communication., 1999.
- [2] S. Haykin, "Cognitive Radio: Brain-Empowered Wireless Communications," in IEEE JSAC, vol. 23, no. 2, pp. 201-220, Feb. 2005.
- [3] The Federal Communications Commission (FCC), "Notice for Proposed Rulemaking (NPRM 03 322): Facilitating Opportunities for Flexible, efficient, and Reliable Spectrum Use Employing Spectrum agile Radio Technologies", T Docket No. 03 108, Dec 2003.
- [4] M. McHenry, "Frequency Agile Spectrum Access Technologies," in FCC Workshop on Cognitive Radio, May 19, 2003.
- [5] IEEE 802.22 WG on Wireless Regional Area Networks, "Functional Requirements for the 802.22 WRAN Standard," <http://www.ieee802.org/22/>.
- [6] V. I. Kostylev, "Energy Detection of a Signal with Random Amplitude", IEEE International Conference on Communication, vol. 3, pp. 1606 – 1610, April 2002
- [7] Z. Tian and B. M. Sadler, "Weighted energy detection of ultra-wideband signals," in IEEE 6th Workshop on Signal Processing Advances in Wireless Communications, pp. 1068 – 1072, June 2005.
- [8] W.A.Gardner, "Signal Interception: A Unifying Theoretical Framework for Feature Detection", IEEE Trans. on Communication, vol. 36, no. 8. Aug. 1988.
- [9] D. Cabric, S. M. Mishra, and R. W. Brodersen, "Implementation issues in spectrum sensing for cognitive radios," in Asilomar Conference on Signals, Systems, and Computers, 2004.
- [10] C. Kim, H. S. Kim, and J. Laskar, et al., "WRAN PHY and MAC Proposal for TDD/FDD," doc.: IEEE 802.22-05/0108r0, http://www.ieee802.org/22/Meeting_documents/2005_Nov/22-05-0108-00-0000_ETRI-SEM-GATech_Proposal_Outline.doc
- [11] Y. Hur, W. Woo, J. Park, K. Lim, C.-H. Lee, H.S. Kim, and J. Laskar, "A wideband Multi-Resolution Spectrum Sensing (MRSS) Technique for A Cognitive Radio (CR) Access System," in 2006 IEEE Int. Symp. On Circuits and Systems (ISCAS 2006), Kos, Greece, May 2006.
- [12] S. Qian and D. Chen, Joint Time-Frequency Analysis: Method and Application, Prentice Hall, 1996.
- [13] B. Razavi, RF Microelectronics, Prentice Hall, 1998